Modeling Steady State Creep in Functionally Graded Thick Cylinder Subjected to Internal Pressure.

Tejeet Singh, V.K. Gupta*

Department of Mechanical Engg, SBS College of Engg & Tech, Ferzoepur-152001, India
*Department of Mechanical Engg, UCOE, Punjabi University, Patiala

ABSTRACT

The steady state creep behavior in an isotropic functionally graded composite cylinder, subjected to internal pressure has been investigated. The cylinder is assumed to be made of composite containing silicon carbide particles in a matrix of pure aluminium. The effect of imposing linear particle gradient on the distribution of stresses and strain rates in the composite cylinder has been investigated. The study reveals that for the assumed linear particle distribution, the radial stress decreases throughout the cylinder with increase in particle gradient, whereas the tangential, axial and effective stresses increases significantly near the inner radius but show significant decrease towards the outer radius. The strain rates in the composite cylinder could be reduced significantly by employing gradient in the distribution of reinforcement.

Key words: Modeling, Cylinder, Creep, Composite, Functionally Graded Material.

1 INTRODUCTION

FGMs are composite materials where the composition is tailored to obtain desired variation in properties. FGMs have been developed as ultra high temperature resistant materials for potential applications in aircrafts, space vehicles and other structural components exposed to elevated temperature [1]. In recent years, the problem of creep in cylinders made of FGMs and operating under high pressure and temperature has attracted the interest of many researchers. Fukui and Yamanaka [2] investigated the effects of the gradation of components on the strength and deformation of thick walled Functionally Graded (FG) tubes under internal pressure. Chen *et al* [3] studied the creep behavior of thick walled cylinders made of FGM and subjected to both internal and external pressures. They obtained the asymptotic solutions on the basis of a Taylor expansion series and compared it with the results of Finite Element analysis (FEA) obtained by using ABAQUS software. You *et al* [4] analyzed the steady state creep in thick walled cylinders made of arbitrary FGMs and subjected to internal pressure. The impact of radial variations of material parameters on the stresses in the cylinder was investigated. Abrinia *et al* [5] obtained analytical solution for computing the radial and circumferential stresses in a thick FG cylindrical vessel under the influence of internal pressure and temperature. In the light of this, it is decided to investigate steady state creep in a thick walled FG cylinder consisting of silicon carbide particles (SiCp) embedded in Aluminium (Al) matrix and subjected to high pressure and temperature.

2 DISTRIBUTION OF REINFORCEMENT

The silicon carbide particle in Functionally Graded composite cylinder has been assumed to decrease linearly from the inner (*a)* to outer radius (*b)*. The content (*vol* %) of silicon carbide *V(r)* at any radius *r* is given by;

$$V(r) = V_{\max} - \frac{(r-a)}{(b-a)}\left[V_{\max} - V_{\min}\right] \qquad (1)$$

where, V_{max} and V_{min} are the maximum and minimum particle content, at the inner and outer radii of the cylinder.
The average particle content in the cylinder of length *'l'* can be expressed as;

$$V_{avg} = \frac{\int_a^b 2\pi r l V(r)dr}{\pi(b^2 - a^2)l} \qquad (2)$$

Putting the value of *V(r)* from Eqn. (1) into Eqn. (2) and integrating, we get,

$$V_{\min} = \frac{3V_{avg}(1-\alpha^2)(1-\alpha) - V_{\max}(1-3\alpha^2+2\alpha^3)}{(2-3\alpha+\alpha^3)} \qquad (3)$$

where, $\alpha = a/b.$

3 ESTIMATION OF CREEP PARAMETERS

In aluminium matrix composites, undergoing steady state creep, the effective creep rate, $\dot{\varepsilon}_e$, is related to the effective stress, σ_e, through well documented creep law based on threshold stress [6],

$$\dot{\varepsilon}_e = A^{'} \left(\frac{\sigma_e - \sigma_0}{E} \right)^n \exp\left(\frac{-Q}{RT} \right) \quad (4)$$

where the symbols $A^{'}$, n, Q, E, R and T denote respectively the structure dependent parameter, true stress exponent, true activation energy, temperature dependent young's modulus, gas constant and operating temperature. A stress exponent of 5 is chosen in this study to describe steady state creep behavior of the composite cylinder.

4 ESTIMATION OF CREEP PARAMETERS

The creep law given by Eqn. (4) may alternatively be written as;

$$\dot{\varepsilon}_e = \left[M \{ \sigma_e - \sigma_o \} \right]^n \quad (5)$$

where $M = \frac{1}{E} \left(A^{'} \exp \frac{-Q}{RT} \right)^{1/n}$ is a creep parameter and the value of stress exponent (*n*) is taken 5 in the current study.

The creep parameters *M* and σ_o appearing in Eqn. (5) are dependent on the type of material apart from the operating temperature (*T*). In a composite, the dispersoid size (*P*) and content (*V*) are the primary material variables affecting these parameters. In the present study, the values of *M* and σ_0 have been extracted from the experimental creep results reported by Pandey *et al* [7] for Al-SiC_P composite under uniaxial creep. The individual set of creep data reported by Pandey *et al* [7] have been plotted as $\dot{\varepsilon}^{1/5}$ versus σ on linear scales. The slope and intercepts of these graphs yield the values of creep parameters *M* and σ_o as reported in Table-1.

Table-1: Creep parameters used for Al-SiC_P

***P* (*μm*)**	***T* (^0C)**	***V* (vol%)**	***M* ($s^{-1/5}$/MPa)**	**σ_o (*MPa*)**
1.7 14.5 45.9	350	10	4.35E-03 8.72E-03 9.39E-03	19.83 16.50 16.29
1.7	350	10 20 30	4.35E-03 2.63E-03 2.27E-03	19.83 32.02 42.56
1.7	350 400 450	20	2.63E-03 4.14E-03 5.92E-03	32.02 29.79 29.18

To estimate the values of *M* and σ_0 for various combinations of *P*, *V* and *T*, not covered in Table 1, regression analysis was performed using Datafit Software. The developed regression equations are given below;

$$M = 0.0287611 - \frac{0.00879}{P} - \frac{14.02666}{T} + \frac{0.032236}{V(r)} \quad (6)$$

$$\sigma_o = -0.084P - 0.0232T + 1.1853(V(r)) + 22.207 \quad (7)$$

In a FG cylinder, with particle content varying radially as *V(r),* both the creep parameters *M* and σ_0 will also vary along the radial direction. In the present study, the particle size (*P)* is assumed as *1.7 μm* while the operating temperature (*T)* is taken as 350 ^oC. The values of *M (r)* and σ_0 *(r)* at any radius, *r*, could be estimated by substituting the particle content *V(r)* at the corresponding locations into Eqs. (6) and (7).

5 MATHEMATICAL FORMULATIONS

Consider a long, closed end, thick-walled, hollow cylinder made of functionally graded Al-SiCp composite. The inner and outer radii of cylinder are respectively *a* and *b* and the cylinder is subjected to internal pressure *p*. The coordinates axes *r, θ* and *z* are taken respectively along the radial, tangential and axial directions of the cylinder. The present analysis is based on the following assumptions;

i. Material of the cylinder is locally isotropic and stresses at any point in the cylinder remain constant with time.
ii. Elastic deformations are small, therefore, neglected as compared to creep deformations.

The radial ($\dot{\varepsilon}_r$) and tangential ($\dot{\varepsilon}_\theta$) strain rates in a cylinder are respectively given by;

$$\dot{\varepsilon}_r = \frac{d\dot{u}_r}{dr} \quad (8)$$

$$\dot{\varepsilon}_\theta = \frac{\dot{u}_r}{r} \quad (9)$$

where $\dot{u}_r = \frac{du}{dt}$ is the radial displacement rate.

Eliminating $\dot{u}_r$ from Eqs. (8) and (9),

$$r \frac{d\dot{\varepsilon}_\theta}{dr} = \dot{\varepsilon}_r - \dot{\varepsilon}_\theta \quad (10)$$

Considering the equilibrium of forces acting on an element of the cylinder in the radial direction, we may write,

$$r \frac{d\sigma_r}{dr} = \sigma_\theta - \sigma_r \quad (11)$$

where σ_r *and* σ_θ are respectively the radial and tangential stresses in the cylinder.

Assuming material of the cylinder to be incompressible, *i.e.*

$$\dot{\varepsilon}_r + \dot{\varepsilon}_\theta + \dot{\varepsilon}_z = 0 \quad (12)$$

where $\dot{\varepsilon}_Z$ is the axial strain rate.

The generalized constitutive equations for creep in an isotropic composite [8], when reference frame is along the principal directions r, θ and z, are given by,

$$\dot{\varepsilon}_r = \frac{\dot{\varepsilon}_e}{2\sigma_e}[2\sigma_r - \sigma_\theta - \sigma_z] \quad (13)$$

$$\dot{\varepsilon}_\theta = \frac{\dot{\varepsilon}_e}{2\sigma_e}[2\sigma_\theta - \sigma_z - \sigma_r] \quad (14)$$

$$\dot{\varepsilon}_z = \frac{\dot{\varepsilon}_e}{2\sigma_e}[2\sigma_z - \sigma_r - \sigma_\theta] \quad (15)$$

According to Von-Mises yield criterion , the effective stress in an isotropic cylinder is given by,

$$\sigma_e = \frac{1}{\sqrt{2}}[(\sigma_\theta - \sigma_z)^2 + (\sigma_z - \sigma_r)^2 + (\sigma_r - \sigma_\theta)^2]^{1/2} \quad (16)$$

For a closed end cylinder made of incompressible material, the plane strain condition exists *i.e.* the axial strain rate $(\dot{\varepsilon}_z)$ is zero. Therefore, Eqs. (8), (9) and (12) on simplifying yields,

$$\dot{u}_r = \frac{C}{r} \quad (17)$$

where C is a constant of integration.

Substituting Eqn. (17) into Eqs. (8) and (9), we get,

$$\dot{\varepsilon}_r = -\frac{C}{r^2} \quad (18)$$

$$\dot{\varepsilon}_\theta = \frac{C}{r^2} \quad (19)$$

Under plane strain condition, Eqn.(15) becomes,

$$\sigma_z = \frac{\sigma_r + \sigma_\theta}{2} \quad (20)$$

Using Eqn. (20) into Eqn. (16), one gets,

$$\sigma_e = \frac{\sqrt{3}}{2}\left(\sigma_\theta - \sigma_r\right) \quad (21)$$

Substituting Eqs. (18) and (20) into Eqn.(13) we get,

$$\sigma_\theta - \sigma_r = \frac{4}{3}\left(\frac{\sigma_e C}{\dot{\varepsilon}_e r^2}\right) \quad (22)$$

Putting $\dot{\varepsilon}_e$ and σ_e respectively from Eqs. (5) and (21) into above equation and simplifying, one gets,

$$\sigma_\theta - \sigma_r = \frac{I_1(r)}{r^{2/n}} + I_2(r) \quad (23)$$

where,

$$I_1 = \left[\frac{2}{\sqrt{3}}\right]^{\frac{n+1}{n}}\left(\frac{C^{1/n}}{M(r)}\right) \quad \text{and,} \quad I_2 = \frac{2}{\sqrt{3}}\sigma_o(r)$$

Using Eqn. (23) into Eqn. (11) and integrating the resulting equation between limits *a* to *r*, we get,

$$\sigma_r = \int_a^r \frac{I_1(r)}{r^{\frac{n+2}{n}}}dr + \int_a^r \frac{I_2(r)}{r}dr + (\sigma_r)_{r=a} \quad (24)$$

The boundary conditions for a cylinder subjected to internal pressure are given by,

(i) At $r = a$, $\sigma_r = -p$ (25)

(ii) At $r = b$, $\sigma_r = 0$ (26)

The Eqn.(24) may be solved, between limits *a* to *b* and under the boundary conditions given above, to get the constant C as,

$$C = \left[\frac{p - \left(2/\sqrt{3}\right)X_1}{\left(2/\sqrt{3}\right)^{\frac{n+1}{n}} X_2}\right]^n \quad (27)$$

where $X_1 = \int_a^b \frac{\sigma_0(r)}{r}dr$ and

$$X_2 = \int_a^b \frac{1}{r^{(n+2)/n}.M(r)}dr$$

Using Eqn. (24) in Eqn. (23), the tangential stress, σ_θ, is obtained as,

$$\sigma_\theta = \int_a^r \frac{I_1(r)}{r^{\frac{n+2}{n}}}dr + \int_a^r \frac{I_2(r)}{r}dr + \frac{I_1(r)}{r^{2/n}} + I_2(r) - p \quad (28)$$

Substituting Eqs. (24) and (28) into Eqn. (20), we get the axial stress, σ_z,

$$\sigma_z = \int_a^r \frac{I_1(r)}{r^{\frac{n+2}{n}}}dr + \int_a^r \frac{I_2(r)}{r}dr + \frac{I_1(r)}{2r^{2/n}} + \frac{I_2(r)}{2} - p \quad (29)$$

6 RESULTS AND DISCUSSIONS

On the basis of analysis presented in previous section, numerical calculations have been carried out to obtain the steady state creep behavior of composite cylinder. The results have been obtained for uniform (Non-FGM) and three different FGM cylinders as mentioned in Table 2.

Table-2: Description of Cylinders

Cylinder	(SiC) Content (*vol %*)			(PG) = (V_{max} - V_{min}) *vol %*
	V_{max}	V_{min}	V_{avg}	
Uniform(C1)	15	15	15	0
FGM (C2)	20	11	15	9
FGM (C3)	25	07	15	18
FGM (C4)	30	03	15	27

6.1 Validation

Before discussing the results obtained in this study, it is necessary to validate the analysis carried out. To accomplish this task, following present analysis the effective strain rates have been computed for a copper cylinder, for which the results are reported in literature [9]. The dimensions of cylinder, operating pressure and temperature, and the values of creep parameters used for the purpose of validation are summarized in Table 3.

Table 3: Summary of data used for validation (Johnson *et al* [9])

Cylinder Material : Copper ; a = 25.4 *mm*, b =50.8 *mm;* p = 23.25 *MPa*; T = 250 ^0C
Creep parameters estimated for copper cylinder: $M = 3.271\times10^{-4}\ s^{-1/5}/MPa$, $\sigma_o = 11.32 MPa$

The tangential strain rates thus obtained have been compared with those reported by Johnson *et al* [9]. A good agreement is observed in Figure 1, which validates the analysis presented in this current study.

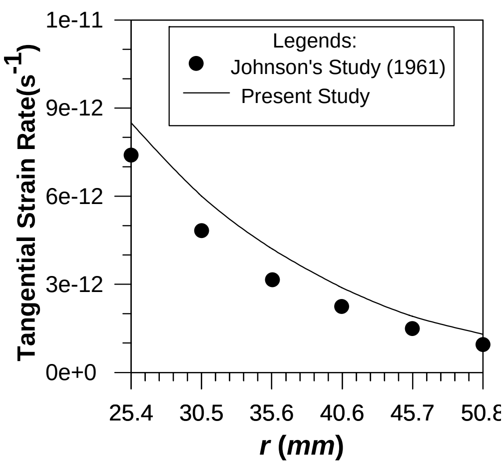

Fig.1 Comparison of strain rates.

6.2. Variation of Creep Parameters

Figure 2 shows the distribution of reinforcement (SiCp) in the various cylinders used in this study. The SiCp content decreases linearly from the inner to outer radius in FGM cylinders(C1-C4) while in uniform (non-FGM) cylinder (C1) the content of SiCp remains the same (15 *vol %*) over the entire radius.

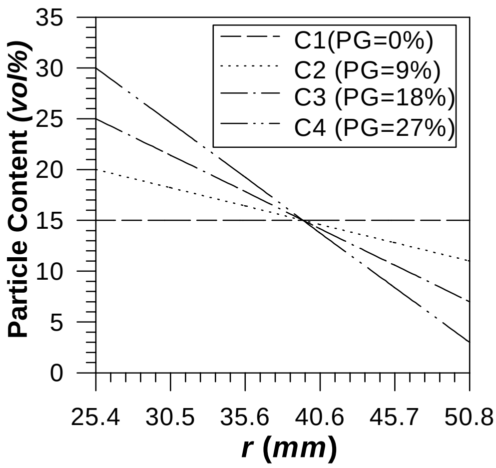

Fig.2 Variuation of particle content.

Figs. 3(a)-(b) show the variation of creep parameters M and σ_0 with radial distance in composite cylinders. The value of parameter M observed in FGM cylinders (C1-C4) increases with increasing radial distance, Figure 3(a). With increase in Particle Gradient (PG), the distribution of M becomes steeper.

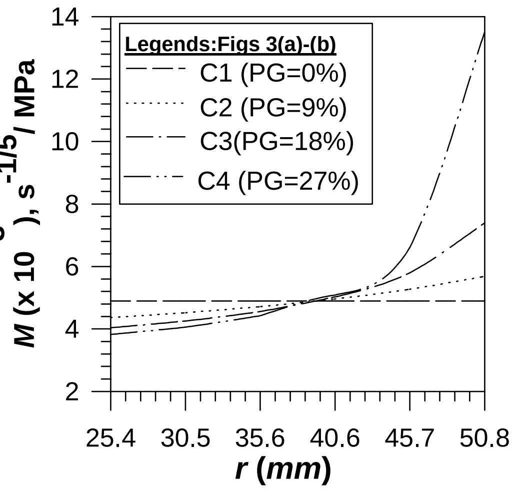

Fig.3(a) Variation of creep parameter '*M*'

On the other hand, the threshold stress, σ_0, shown in Figure3(b) decreases linearly on moving from the inner to outer radius of the FGM cylinder. The creep parameter observed in uniform cylinder (C1) remains constant due to the same amount (15 *vol %*) of SiCp.

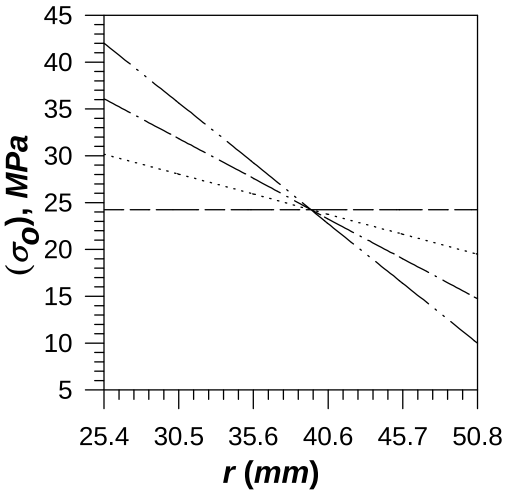

Fig.3(b) Variation of creep parameter σ_o

6.3 Distribution of Stresses and Strain Rates

To observe the effect of particle gradient on creep behavior of cylinder, the steady state stresses and strain rates have been estimated in four different composite cylinders, Table 2, and are shown in Figs. (4)-(5). The magnitude of radial stress, Figure 4(a), decreases throughout the cylinder with increase in particle gradient. The maximum variation noticed in radial stress between FGM cylinder C4 and uniform cylinder C1 is about 8.2*MPa*, somewhere in the middle region.

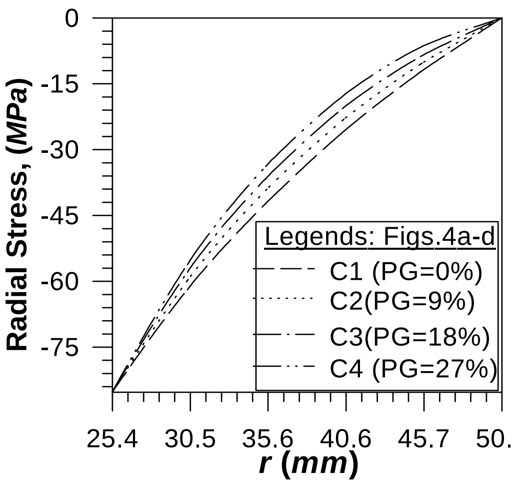

Fig.4 (a) Variation of Radial Stress.

The tangential stress shown in Figure 4(b) remains tensile throughout and is observed to increase with increasing radius. By incorporating more amount of reinforcement (SiCp) near the inner radius (as in FGM cylinder), the tangential stress increases near the inner radius but decreases towards the outer radius when compared with uniform cylinder C1. The location of highest tangential stress shift towards the inner radius with increasing particle gradient beyond 9%, as observed for FGM cylinders C3 and C4

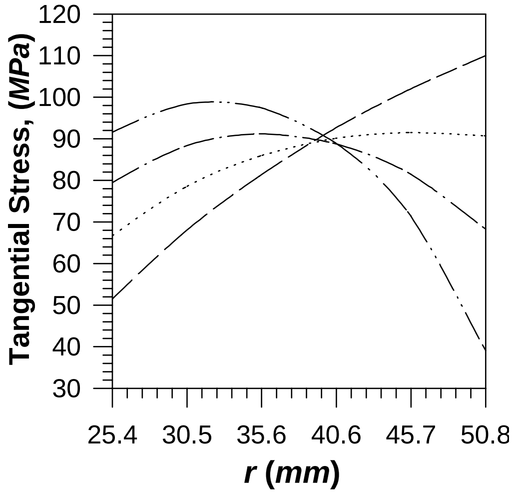

Fig.4(b) Variation of Tangential Stress.

It is interesting to observe that the axial stress changes its nature from compressive (uniform cylinder C1) to tensile (FGM cylinder C4) at the inner radius, Figure 4(c). The maximum axial stress, observed at the outer radius, decreases with increasing particle gradient from 0% to 18%. With further increase in particle gradient to 27%, the location of maxima observed in axial stress shifts towards the middle region of the cylinder (cylinder C4).

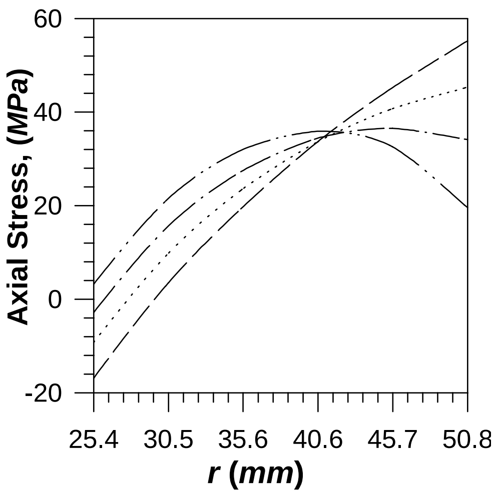

Fig.4(c) Variation of Axial Stress.

The effective stress, Figure 4(d), decreases with increasing radial distance. The increase in particle gradient in the composite cylinder, leads to significant increase in effective stress near the inner radius but a significant decrease near the outer radius.

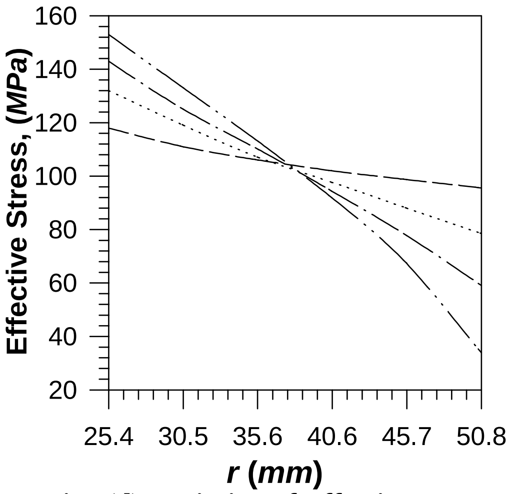

Fig.4(d) Variation of Effective Stress.

The radial and tangential strain rates are equal in magnitude but opposite in nature due to incompressibility condition (Eqn. 12) and the assumption of plain strain condition ($\dot{\varepsilon}_z = 0$).The strain rates in FGM cylinder decreases significantly over the entire radius as evident from Figure5.

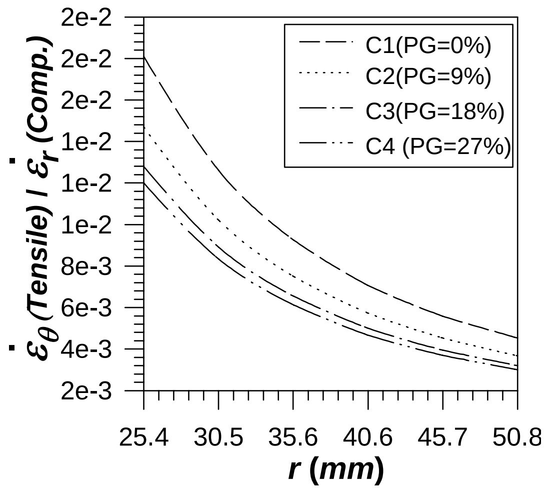

Fig.5 Variation of Strain Rates.

The decrease observed in strain rate increases further with increase in particle gradient. By increasing the content of SiC_P near the inner radius of composite cylinder, the inter-particle spacing decreases which causes the increase in threshold stress (Li and Langdon, 1999)[10] but decrease in creep parameter *M* (Figure 3a). Both these factors contribute in reducing the strain rates near inner radius of FGM cylinders compared to uniform cylinder. But towards the outer radius, in spite of relatively higher value of parameter *M,* the strain rates in FGM cylinder remains lower than the uniform cylinder C1 due to lower value of effective stress observed in FGM cylinders.

7 CONCLUSIONS

The study carried out has led to the following conclusions:

1. The radial stress in the composite cylinder decreases throughout with increasing gradient in the distribution of reinforcement. The increase in particle gradient leads to increase in tangential, axial and effective stresses near the inner radius but decrease at the outer radius.

2. The location of maxima observed for tangential stress shifts towards the inner radius as well as its magnitude increases with increasing particle gradient.

3. By employing gradient in the distribution of reinforcement, the strain rates in the composite cylinder could be reduced to a significant extent over the entire radius.

References

[1] Noda, N., Nakai, S., Tsuji, T. Thermal stresses in functionally graded materials of particle- reinforced composite. JSME Int J Series A. 1998; 41(2): 178-184.

[2] Fukui, Y., Yamanaka, N. Elastic Analysis for Thick-Walled Tubes of Functionally Graded Material Subjected to Internal Pressure. JSME Int J Series I. 1992; 35(4): 379-385.

[3] Chen, J.J., Tu, S.T., Xuan, F.Z., Wang, Z.D. Creep analysis for a functionally graded cylinder subjected to internal and external pressure. The J Strain Analysis for Engng Design. 2007; 42(2): 69-77.

[4] You, L.H., Ou, H., Zheng, Z.Y. Creep deformations and stresses in thick-walled cylindrical vessels of functionally graded materials subject to internal pressure. Composite Structure. 2007; 78: 285-291

[5] Abrinia, K., Naee, H., Sadeghi, F., Djavanroodi, F.. New analysis for the FGM thick cylinders under combined pressure and temperature loading. American J of Applied Sc. 2008; 5 (7): 852-859.

[6] Tjong, S.C., Ma, Z.Y. Microstructural and mechanical characteristics of in situ metal matrix composites. Mater Sci Engng. 2000; R29 (3-4): 49-113.

[7] Pandey, A.B., Mishra, R.S., Mahajan, Y.R. Steady state creep behavior of silicon carbide particulate reinforced aluminium composites. Acta Metall Mater. 1992; 40(8): 2045-2052.

[8] Gupta, V.K., Singh, S.B., Chandrawat, H.N., Ray, S. Modeling of creep behavior of a rotating disc in presence of both composition and thermal gradients. J Engng Mater Technol. 2005; 127(1):97-105.

[9] Johnson, A.E., Henderson, J., Khan, B. Behavior of metallic thick-walled cylindrical vessels or tubes subjected to high internal or external pressures at elevated temperatures. Proc Instn Mech Engrs. 1961; 175(25): 1043-1069.
[10] Li, Y., Langdon, T.G. An examination of a substructure-invariant model for the creep of metal matrix composites. Mater Sci Engng. 1999a; A265(1): 276–284.
[11] Li, Y., Langdon, T.G. Creep behavior of an Al-6061 metal matrix composite reinforced with alumina particulates. Acta Mater. 1997; 45(11): 4797-4806.